

OPEN ACCESS

\*Corresponding author

Mohammed Dara Kamal  
muhammad.kamal@su.edu.krd

RECEIVED :22 /04 /2025

ACCEPTED :11/08/ 2025

PUBLISHED :28/ 02/ 2026

KEYWORDS:

Reinforced Concrete Corbel, Basalt Fiber-Reinforced Polymer BFRP rebar, Shear strength and Failure mode.

# Experimental Investigation on Shear Behavior of Double Sided Reinforced Concrete Corbels Using BFRP Bars

Mohammed Dara Kamal\* & Sinan Abdulkhaleq Yaseen

Department of Civil Engineering- College of Engineering, Salahaddin University-Erbil, Erbil, Iraq.

## ABSTRACT

A reinforced concrete corbel is a short cantilever structural member extending from columns or walls, resisting mostly vertical loads by shear action. The paper presents an experimental investigation on the shear behavior of reinforced concrete corbels reinforced longitudinally with Basalt Fiber-Reinforced Polymer (BFRP) bars as an alternative material to conventional steel reinforcement. Eight double-sided reinforced concrete corbels measured 180mmx300mm and a central column segment 180mmx300mm, with different longitudinal reinforcement of BFRP ratios (1pb, 1.57pb, 3.15pb, and 5.6pb) and shear span-to-depth ratios ( $a/d = 1.0$  and  $1.25$ ) were tested under an experimental program. In specimens with  $a/d = 1.0$ , an increase in reinforcement ratio to 5.6pb resulted in an ultimate shear strength increase by 34.25%. Nevertheless, at the higher shear span-to-depth ratio ( $a/d = 1.25$ ), the largest shear strength increased about 67.6% at 3.15pb, beyond this ratio, the shear strength significantly decreased to 42.7% at 5.6pb, indicating reaching the optimal limit. These results validate the efficiency of utilizing BFRP reinforced polymer bars to increase shear capacity in concrete corbels and choosing the reinforcement ratio to induce optimal structural behavior.

## 1. Introduction

A concrete corbel is a short, cantilevered structural extension that projects from a column or wall, often used in precast and cast-in-place concrete construction to support beams or girders. Unlike traditional beams that resist loads mainly through flexure actions, corbels rely mostly on the direct compressive strut action for short span. The design of concrete corbels generally follows two key approaches. The empirical design method is most used when the shear span-to-depth ratio ( $a/d$ ) is less than 1.0, while the strut and tie method (STM) is applied for corbels with a ratio between 1.0 and 2.0. The STM approach characterises internal force transfer through compression struts and tension ties.

Concrete corbels can show different failure modes, namely diagonal compression of the strut, shear-compression failure, and diagonal splitting, all of which are controlled by key parameters such as reinforcement ratio, concrete compressive strength, and load application. Understanding these failure modes is important for optimizing corbel design.

The current method uses a strut-and-tie model, which improves the shear strength predictions for corbels. The Current study investigates the performance of reinforced concrete corbels reinforced with Basalt Fiber Reinforced Polymer (BFRP) bars, offering a corrosion-resistant alternative as a replacement for traditional steel reinforcement. FRP is a composite modern class of materials mostly used as an alternative to traditional steel reinforcement in different types of applications. These Fiber-Reinforced Polymer (FRP) composites are made up of high-strength fibers embedded in a polymer matrix with excellent corrosion resistance and a high strength-to-weight ratio. This makes them highly suitable for structures with severe environmental exposure, which are damaged over time. Unlike steel, FRP materials exhibit linear-elastic stress-strain behavior with no definite yield stage by (Abbood et al., 2021).

The shear behavior of reinforced concrete corbels has been studied thoroughly various parameters influence the strength. The study of (Dang et al., 2024) Investigated the performance of four GFRP-reinforced concrete corbels with dimensions 200mmx250mm by increasing the longitudinal reinforcement ratio  $\rho_f = 0.56\%$  and  $\rho_f = 0.87\%$ , and it was concluded that greater reinforcement ratios lead to enhanced shear behavior of the concrete corbel and overall shearing resistance. The shear span to depth ratio ( $a/d$ ) was also categorized as a significant parameter, and experiments showed that any increase in  $a/d$  causes a corresponding decrease in shearing strength due to a change in the mode of failure studied by (Dawood and Abdul-Razzaq, 2018).

(Abu-Obaida et al., 2018) investigated the structural behavior of concrete corbel internally reinforced with Glass Fiver Reinforced Polymer GFRP bars testing of 12 specimens with dimension 150mmx300mm with shear span to depth ratio less than or equal to 2, increasing the longitudinal reinforcement ratio of GFRP shifted the failure mode from diagonals strut to splitting failure, at reinforcement ratio of 7.5pb with high concrete strength 40 MPa shear strength reduced due to splitting failure. And the reduction in shear strength observed when the shear span to depth ratio decreased  $a/d$ .

Another influence parameter was compressive concrete strength also significant role in shear strength, as increased strength increases the diagonal strut mechanism and the effects of confinement, which results in better shearing capacity of the corbels reported by (Lu et al., 2009).

## 2. Research Significance

The study investigates the behavior of eight reinforced concrete corbels reinforced with basalt FRP bars with variable reinforcement ratio and shear-to-depth ratio. The major variables investigated in this study included:

- Failure modes,
- Load deflection response
- Load concrete strain response
- Load BFRP strain response

### 3. Methodology

#### 3.1 Corbel Specimen

This experiment studied 8 doubly-sided reinforced concrete corbels, each attached to a central column. **Figure 1** represents the geometrical layout for all specimens. The corbels were classified into two major groups according to the  $a/d$ . Based on the  $a/d$ -ratio, the BFRP-reinforced corbels belonged to the first category of 1.0 and 1.25. Each corbel measured 180mm in width and 300mm in

height, and was cast monolithically with the central column segment of dimensions 180x300mm. These columns were reinforced by 4 BFRP bars of diameter 12 mm, while the stirrups, only serving as holders in the columns, had a 6 mm diameter ( $\phi 6$ ). Supports were extended to improve anchorage, and the beams were fitted with closed BFRP stirrups ( $\phi 6$ ) to avoid slipping of the BFRP reinforcement.

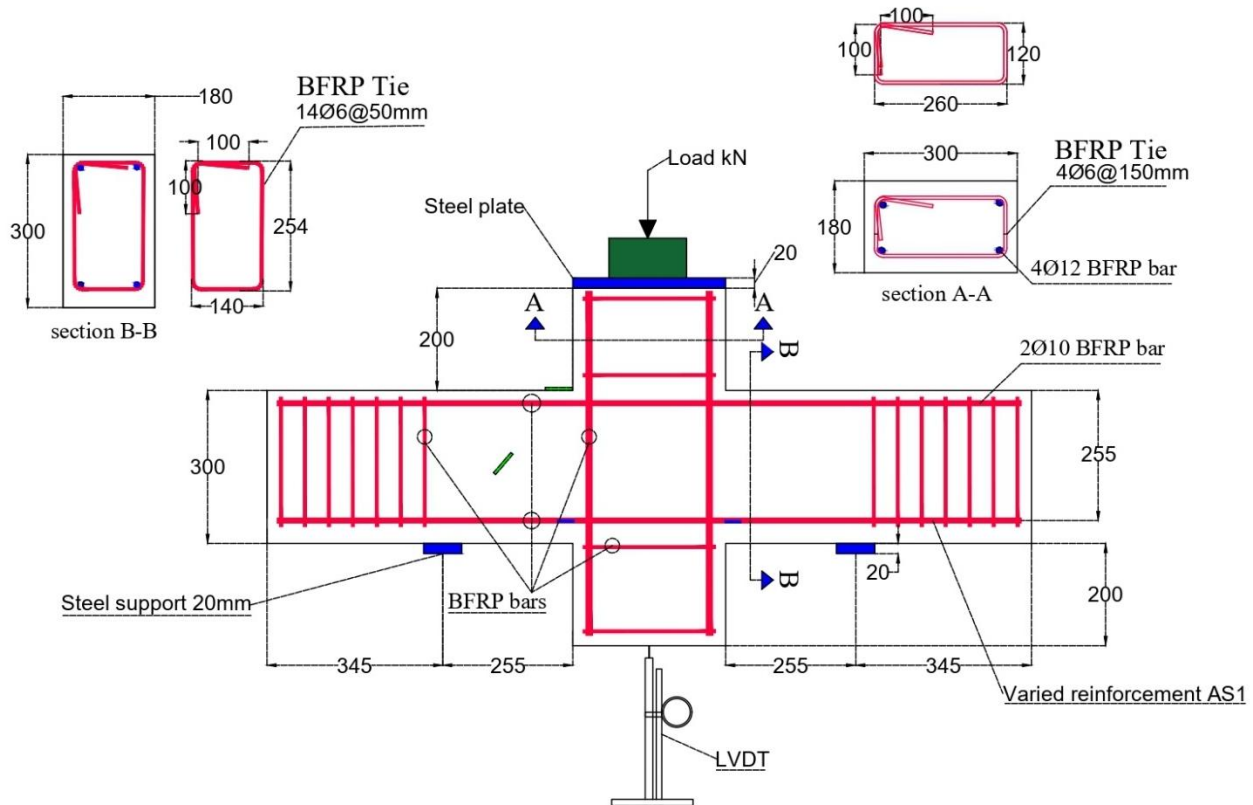


**Figure 1.** Double side of reinforced concrete corbel details dimension in mm ( $a = 270\text{mm}$  for  $a/d = 1$   $a = 332\text{mm}$  for  $a/d = 1.25$ , — Concrete 50mm strain gauge — BFRP 3mm strain gauge)

#### 3.2 Corbel Specimen

As summarized in **Table 1**, the experimental program involved eight double-sided reinforced concrete corbels to examine their structural behavior with different types and arrangements of reinforcement. Eight specimens were cast with ready mix concrete having compressive strengths  $f_c = 30\text{MPa}$  and a mix design proportion of the concrete

present in **Table 2**. The specimens were varied in terms of reinforcement type (BFRP or steel bars), shear span-to-effective depth ratio ( $a/d = 1.0$  and  $1.25$ ), and the reinforcement ratios following the recommendation of (ACI Committee 440 2015). All specimens were designed to be over-reinforced, ratio of longitudinal reinforcement to balance reinforcement  $\rho_f / \rho_b > 1.4$  to ensure that the failure mode was caused by the crushing of

concrete, before rupture of the primary BFRP reinforcement. The longitudinal reinforcement ratio adopted for the experimental specimens is 1pb, 1.57pb, 3.15pb, and 5.6pb.

The BFRP-reinforced corbels were reinforced using 10mm, 12mm, and 16mm bars in diameter. A loading test was conducted on every specimen, and the load was applied at the top of the column to simulate real structural conditions. The two ends of the corbels were supported, and the load was incremented using a hydraulic actuator until failure. Linear Variable Differential Transformers (LVDT)

were installed to measure vertical deflections at the tip of the corbel, and strain gauges were used with a resistance of around 120 Ohms on the reinforcement bars to measure the development of strain under load. The load was read using the camera on the machine monitor, and the strain gauges were connected to the special data logger, which was connected to a computer; the data logger recorded and saved all data (FRP strains, concrete strains).

**Table1.** Experimental specimens of reinforced concrete corbels

Group	a/d ratio	BFRP reinforcement ratio	Reinforcing bars (AS1)	Name	P <sub>exp</sub> (kN)	V <sub>exp</sub> (kN)	First Crack (kN)	Deflection (mm)	First Shear Crack (kN)	Failure Mode
C30	1	1pb	2Ø10	C30-R1-pb1-F	400	200	68	10.000	154	F
		1.57pb	2Ø12	C30-R1-pb1.57-F	450.5	225	73	10.418	162	DC
		3.15pb	4Ø12	C30-R1-pb3.15-F	478.9	239	82	5.475	153	DC
		5.6pb	4Ø16	C30-R1-pb5.6-F	537.0	269	89	3.800	154	DC
	1.25	1pb	2Ø10	C30-R1.25-pb1-F	290.4	145	58	18.004	153	F
		1.57pb	2Ø12	C30-R1.25-pb1.57-F	255.1	128	57	10.068	129	DC
		3.15pb	4Ø12	C30-R1.25-pb3.15-F	427.5	214	60	8.958	117	SP
		5.6pb	4Ø16	C30-R1.25-pb5.6-F	244.9	122	64	3.805	110	SP

**Table 2.** Concrete mix proportion

Mix proportion	SSD kg/m <sup>3</sup>	Weight of Wet Basis kg
mixing water (dry / wet)	1	106
water / cement ratio	-	0.29
cement	3.15	360
Coarse gravel	2.70	526
Fine gravel	2.70	349
Fine aggregates (sand)	2.62	1074
Total weight & volume 1 m <sup>3</sup>		2417

### 3.3 Materials

The compressive strength test was conducted as per ASTM C39/C39M-23 for cylindrical test specimens of concrete. Standard-sized 150×300 mm test pieces were molded, left to cure for 28 days, and finished in their smooth and perpendicular state through grinding or capping in sulfur. Each specimen was tested in a compression machine after 28 days, as summarized in **Table 3**.

The tensile strength testing for BFRP (basalt fiber reinforced polymer) rebar, as specified by ASTM d7205/d7205M, involves preparing samples with a free length of at least 40 times the effective diameter (minimum 400 mm) and attaching end tabs (100 mm long) at both ends using high-strength (epoxy sika anchor fix 3030). The inner diameter of the end is slightly larger than the rebar diameter (10.5 mm for 10 mm rebar, 12.5 mm for 12 mm rebar, 16.5 mm for 16 mm rebar), while the outer diameter after epoxy application is approximately 1 mm larger (11.5 mm for 10 mm rebar). The specimen is then placed in a testing machine. The ultimate tensile strength is determined by dividing the peak force by the nominal cross-sectional area. Ensuring proper alignment and secure gripping is crucial to prevent premature failure at the grips. **Table 4** show the tensile strength of different sizes of BFRP rebar. The mechanical properties of BFRP bars used in this study were tested to determine their structural behavior.

**Table 3.** Compressive strength of specimen concrete corbels

Number	Length (mm)	Diameter (mm)	Load (kN)	Strength (MPa)	Average
1	300	150	590	33.4	32.15
2	300	150	554	31.36	
3	300	150	560	31.7	

**Table 4.** Mechanical properties of BFRP rebar

Bar Diameter	Modulus of elasticity (GPa)	Ultimate tensile strength (MPa)	Ultimate Strain
10	46	946	0.02135
12	48	977.2	0.0208
16	45	754	0.018

### 3.4 Setup and Equipment

The test setup involved testing all specimens to failure under displacement-controlled loading at a rate of 3 kN/sec increment. The load was applied to the top surface of the column segment by a (UNIVERSAL) machine with a 1200-kN load capacity. The specimens were placed on two steel pedestals to impose boundary conditions. A 1000-kN load cell measured the applied load precisely during the test. To measure deflection, a linear variable differential transducer (LVDT) was positioned at the midpoint of the bottom surface of the column segment, and the maximum capacity to measure was about 80mm. Concrete strain gauges with a 50-mm gauge length were installed on the concrete surface, as shown in **Figure 2**, at the critical surface of maximum moment (near the top beam-column junction) and diagonal strut compression areas. Strain gauges with a 3-mm gauge length were also installed on BFRP reinforcing bars at sections of maximum stress to measure their strain response during loading. All data, including load, deflection, and strain readings, were measured by a high-precision data logger system, which provided full and precise data collection for analysis. This setup allowed close observation of the structural behavior and failure mechanism of the specimens under investigation.



**Figure 2.** a) 50mm concrete strain gage, b) 3mm BFRP strain gauge

## 4. Results and Discussion

### 4.1 Failure Mode

Three failure modes were observed in the BFRP reinforced concrete corbels examined in this study, as illustrated in **Figure 3 (a)**, first flexural failure (F) occurs due to low reinforcement ratio and was characterized by the initiation of cracking at the corbel - column junction and propagate towards, the longitudinal reach ultimate tensile strength limit without yielding, due to linear relation stress strain curve of FRP materials. diagonal compression failure (DC) in **Figure 3 (b)** by crushing of concrete in diagonal strut region by excessive compressive stress and the form of inclined crack occur between support and top column beam junction. In **Figure 3 (c)**, at high reinforcement ratio, the development of radial tensile stress around BFRP rebar reinforcement exceeded the tensile strength of the concrete and resulted in longitudinal cracking along the reinforcement, leading to the splitting tensile failure.

The experimental result presented in **Table 1** shows that the failure modes of all specimens were significantly influenced by BFRP reinforcement ratio and shear span to depth ratio ( $a/d$ ) the main inclined crack ranging from 27% to 52%. For C30-R1-pb1-F with pb1 and the  $a/d = 1$ , inhibited flexural failure. Crack propagation initiated at the corbel-column joint, where the moment is high, and

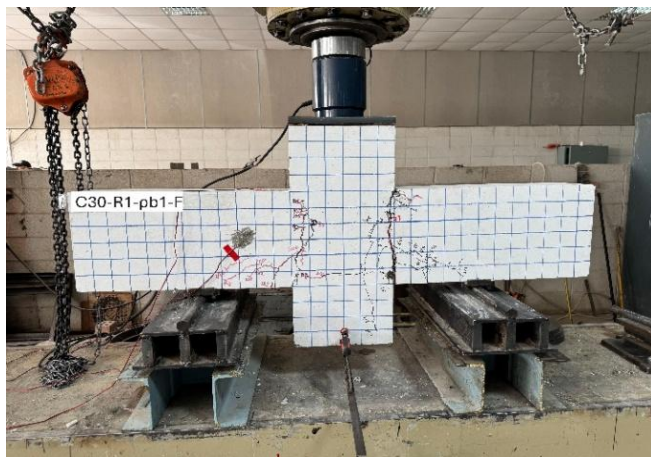
propagated towards the load point. As loading increased incremental, the longitudinal BFRP reinforcement reached the elastic limit and failed by Flexural failure, the same failure noted by (Ali and Mahdi, 2015).

All other specimens, which were C30-R1-pb1.57, C30-R1-pb3.15-F, and C30-R1-pb5.6-F, were reinforced with high reinforcement ratios ranging from 1.57pb, 3.15pb, and 5.6pb, respectively. Also failed in diagonal compression and the first inclined crack within 28.6% to 35.9% of the ultimate load, the failure was due to crushing of the concrete strut by the development of internal arching action exceeding the compressive strength. This finding is in agreement with compression strut crushing after internal arching action reported by (Ridha et al., 2017).

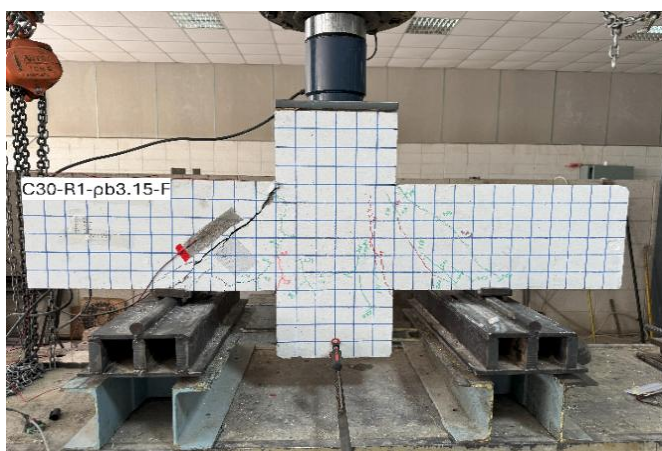
In the group with shear span to depth ratio of  $a/d = 1.25$ , specimen C30-R1.25-pb1-F with low reinforcement flexural failure exhibited. The first initial crack was observed at the corbel column junction and developed vertically significantly, indicating bending behavior and shear crack developed at 50.5% of the main load, due to increasing shear span to depth ratio to 1.25 reduced the effect of internal arching mechanism. This observation aligned with (Al-Kamaki et al., 2018) reported that the increase of  $a/d$  enhances the flexural failure modes in concrete corbels.

In the specimen C30-R1.25-pb1.57-F failure mode transitioned to DC failure, and the first diagonal shear crack was observed at 52.5% of the ultimate load. Specimens R1.25-pb3.15-F and C30-R1.25-pb5.6-F exhibited splitting failure (SP), due to tensile stress developed perpendicular to the principal load path, which exceeded the tensile strength of concrete.

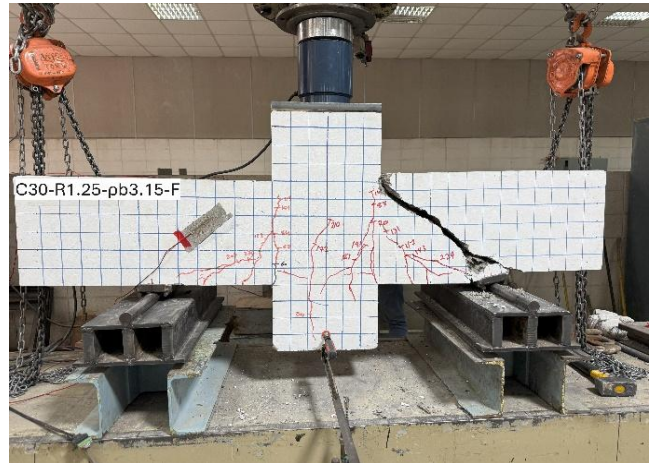
The major factor depended on increasing the reinforcement ratio, a lack of adequate transverse reinforcement. Similar splitting failures have also been observed by (Kheyroddin et al., 2024) and (Canha et al., 2014) in the case of FRP-reinforced corbels, most significantly in the case of high reinforcement ratios and high shear.



a) Flexural Failure (F)



b) Diagonal strut crushing (DC)



c) Diagonal Splitting (SP)

Fig. 3. Failure mode of concrete corbels

#### 4.2 Load and Deflection

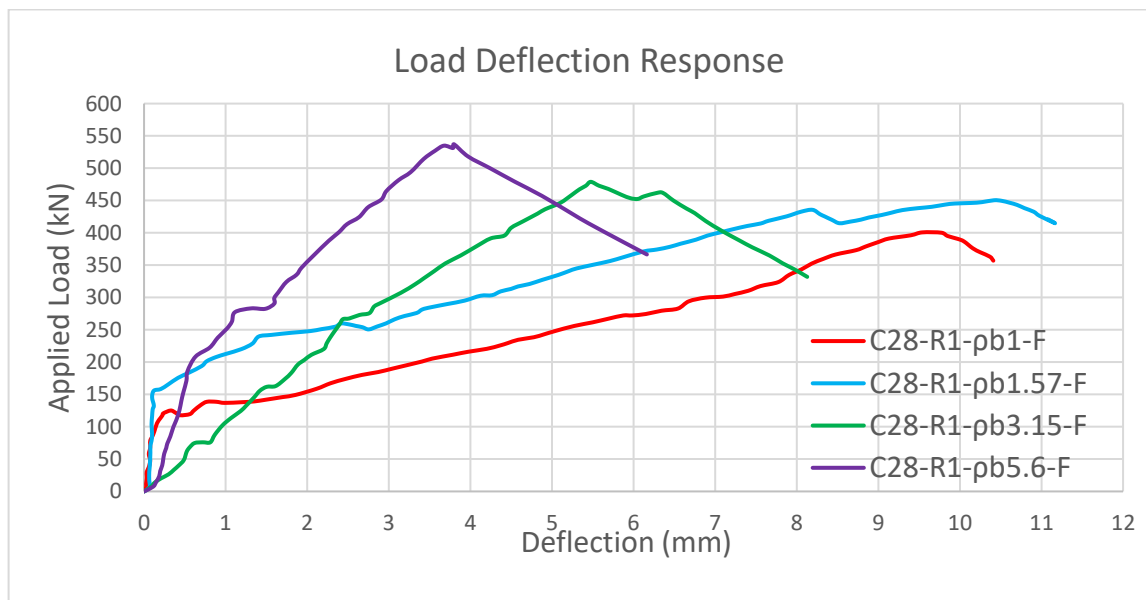
The experimental results in **Figure 4** illustrate the load-deflection curve of double-sided concrete corbels with different shear span-to-depth ratios ( $a/d = 1.0$  and  $1.25$ ) and varying reinforcement ratios. For the specimens with an  $a/d$  ratio of  $1.0$ , increasing the reinforcement ratio from specimen C30-R1-pb1-F to C30-R1-pb5.6-F resulted in a notable enhancement in load capacity, accompanied by a reduction in deflection at peak load. Specifically, the load improved by approximately 34.25%, increasing from 400 kN to 537 kN when the reinforcement ratio rose from the lowest value 1pb to the highest 5.6pb. This rise was accompanied by a considerable drop in deflection, falling by almost 62% from about 10 mm to 3.8 mm. The reduced deflection and the improved load capacity reflect increased effectiveness of the compression strut mechanism, and arch action increased the stiffness and reduced the deflection, as greater reinforcement ratios allow better load transmission through concrete compression struts as opposed to the tensile reinforcement. These findings were echoed by Abu-Obaida et al. (2018) who reported that greater ratios of reinforcement moved the main mode of failure towards diagonal compression.

In contrast, in the specimens of  $a/d$  of  $1.25$ , while the increase of the reinforcement ratio from C30-R1.25-pb1-F to C30-R1.25-pb3.15-

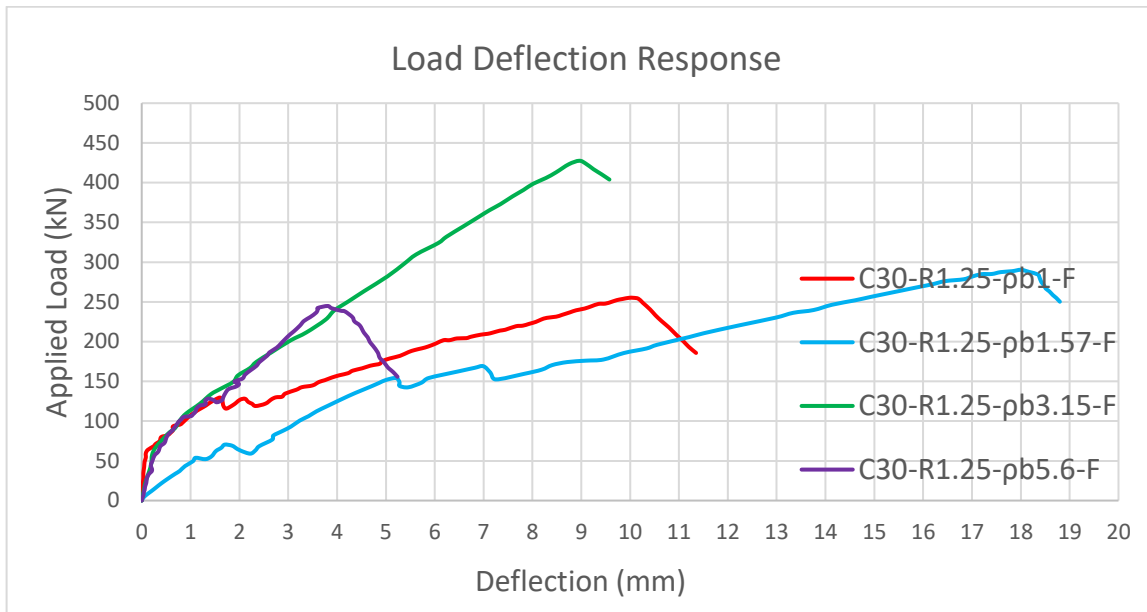
F greatly improved load capacity by about 47%, from 290.4 kN to 427.5 kN, together with reduced deflection by approximately 18 mm to a deflection of about 9 mm. Similar to observations of Dang et al. (2024), it was confirmed that increasing the reinforcement ratio tends to increase the diagonal strut mechanism and therefore the load-carrying capacity to a certain optimal value. But beyond this point, further increase to a value of the reinforcement ratio of 5.6pb for specimen C30-R1.25-pb5.6-F resulted in a large reduction in the load capacity, decreasing approximately 42.7% and load capacity to 244.9 kN, together with significant reductions in the deflection to 3.8 mm. It is reasonable that the strength-reducing loss in strength at very high values of the reinforcement ratio is caused by the resulting internal stresses leading to premature splitting failure; these results integrate with such a splitting failure was also observed by (Abu-Obaida et al., 2018) in their high-strength, high-reinforced GFRP corbels.

In **Figure 5**, the graph shows the effect of the varied a/d ratio on the shear strength of the concrete corbel with different reinforcement ratios. Increasing the a/d from 1 to 1.25 resulted in observed shear strength reductions of 36.22% for specimens with reinforcement ratio 1pb, 35.54% for 1.57pb, 10.74% for 3.15pb, and 54.37% for 5.6pb. These reductions are primarily due to the decreased effectiveness of the arch action mechanism as the a/d increased. The elongated load path in higher a/d specimens increased the stiffness and reduced the flexural stress contribution and leading to splitting failure due to induced perpendicular tensile stress along the diagonal compression path. Obviously, transition from diagonal compression (DC) failure to splitting failure (SP) with increased a/d ratio.

The smaller difference in load capacity for 3.15pb specimens was a more balanced interaction between the BFRP reinforcement ratio and the geometry of the concrete corbel, which effectively sustains the shear strength.



a) group a/d = 1



b) group a/d=1.25

Figure 4. Load and deflection response of groups (a) and (b)

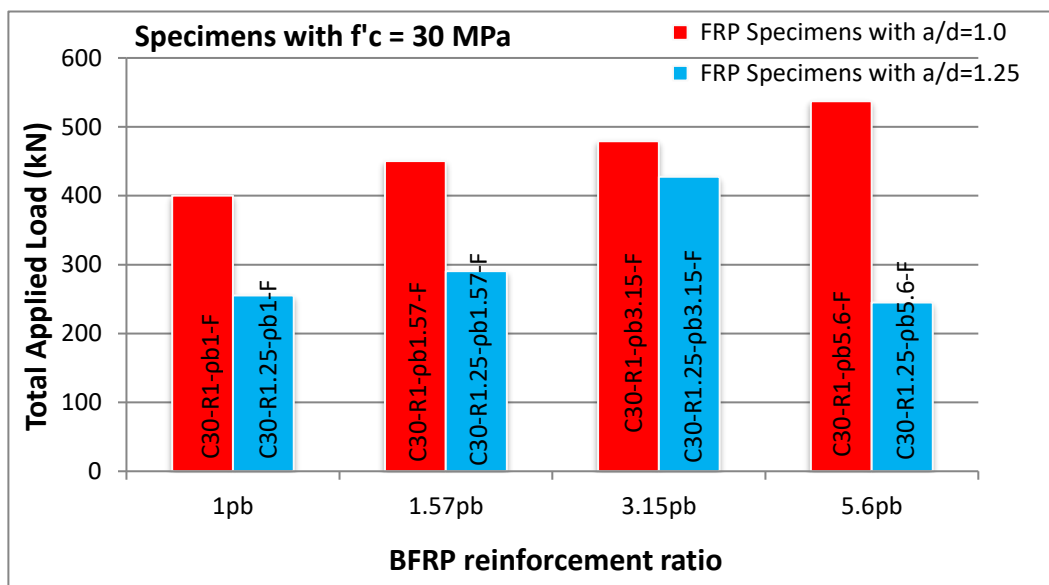


Figure 5. Load capacities between corbel groups

4.3 Concrete Strain

Figure 6(a) shows the load–diagonal concrete strain response of corbel specimens with a shear span-to-depth ratio (a/d) of 1.0. As the reinforcement ratio increased, there was an increase in strain related to the arch action mechanism as a result of developing internal compressive stresses along the diagonal strut. The lowest reinforced ratio specimen, C28-R1-pb1-F, had a diagonal strain of around 263  $\mu\epsilon$  at failure, which was consistent with a

flexural failure mechanism. For this specimen, large strains at the upper concrete resulted from high bending moments developing at the beam–column junction. With an increase in the reinforcement to pb1.57 and pb3.15, there was an increase in diagonal strain values to around 270  $\mu\epsilon$  and 325  $\mu\epsilon$ , respectively. The increase reflects a higher activation of the mechanism of the diagonal strut to transfer stresses at a higher rate across the width of the strut. In an over-reinforced specimen, C28-

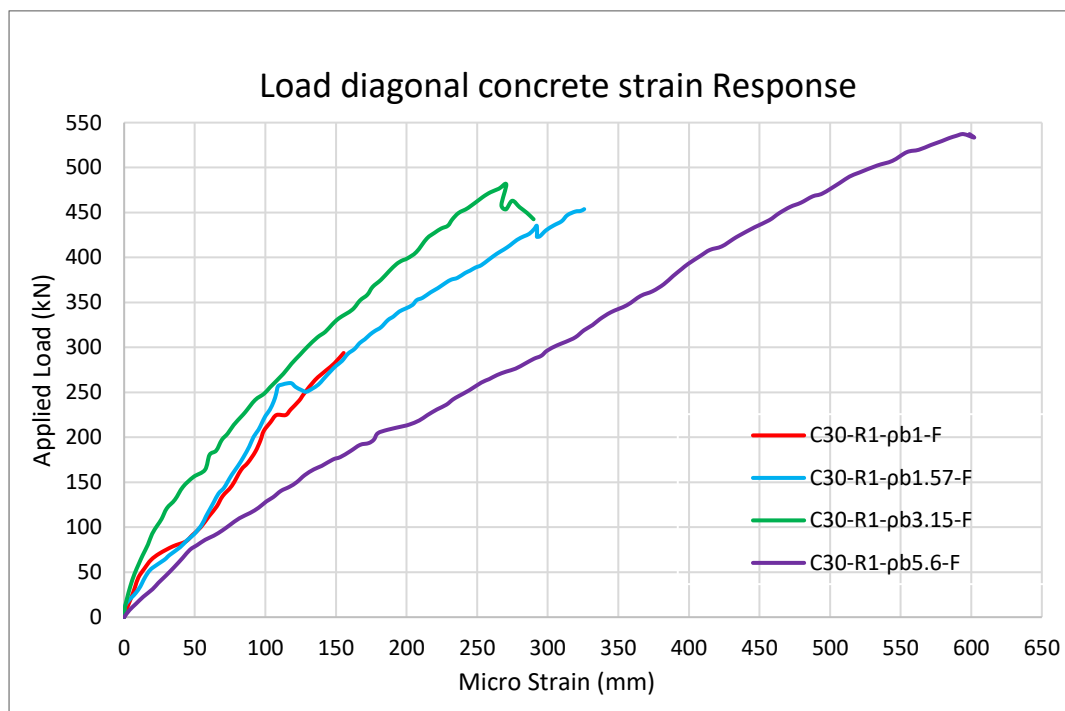
R1-pb5.6-F, there was a large increase in the diagonal strain to around  $602 \mu\epsilon$ , reflecting an increased capacity of the strut and a likely prolongation of failure. Alternatively, this may reflect heavy localization of stress that initiated failure through diagonal compression (DC). Specimen C28-R1-pb5.6-F, with reinforcement ratio, exhibited higher diagonal compression strains at the same level as other specimens in this group. This was primarily due to significant stress concentration, with changing and transition failure to diagonal compression failure by localizing the stresses along the diagonal compression strut.

**Figure 6(b)** shows the load–diagonal concrete strain response for corbel specimens with a higher  $a/d$  ratio of 1.25. All of these specimens exhibited lower diagonal strain compared to the  $a/d = 1.0$  group, illustrating a definite shift in structural response as a result of increased shear span. The maximum diagonal strain for specimen C28-R1.25-pb1-F was around  $247 \mu\epsilon$ , and for those with reinforcement ratios pb1.57 and pb5.6, it was similar at  $217 \mu\epsilon$  and  $337 \mu\epsilon$ , respectively. The declines in these values of diagonal strain arose through reduced effectiveness of the arch action as a

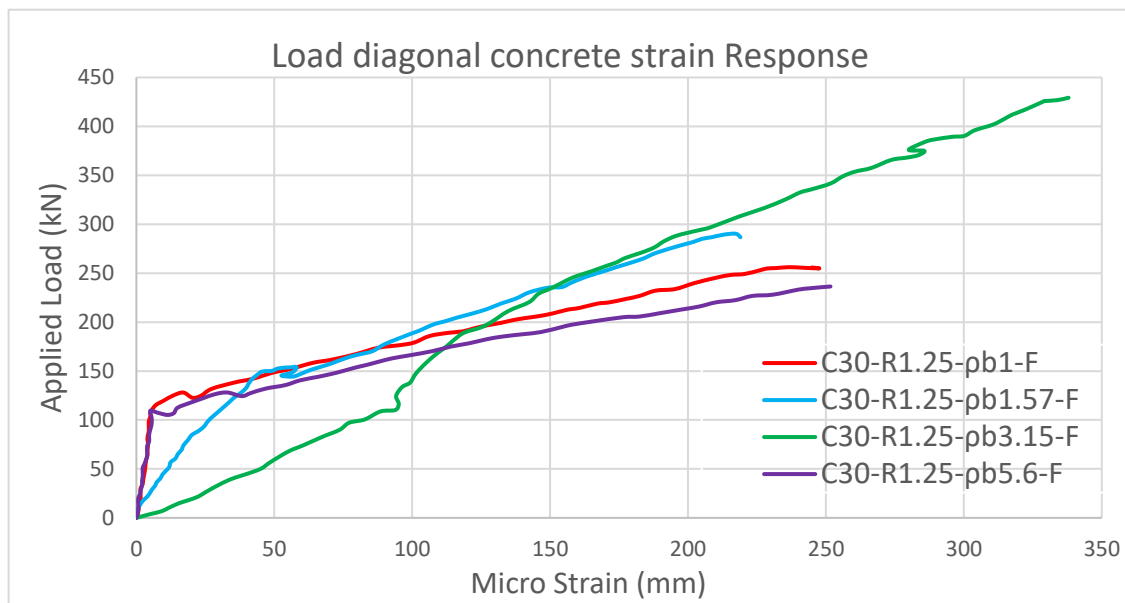
result of increased shear span redirecting internal paths for stress and restricting engagement of the diagonal strut. The maximum of this group, around  $350 \mu\epsilon$ , occurred for C28-R1.25-pb3.15-F and can be attributed to an optimum combination of geometry and reinforcement. In contrast, specimens C30-R1.25-pb1.57-F and C30-R1.25-pb3.15-F showed a rapid initial increase in diagonal compression strain at a lower same load, which was attributed to the increased  $a/d$ , transition in the failure mode from flexural to DC and SP.

Generally reduced strain values for all specimens suggest that for  $a/d = 1.25$ , compression along the diagonal was not a failure mechanism. Instead, strain was contained within the region of the strut, and structural failure likely occurred by concrete cracking or splitting down the diagonal prior to full mobilization of strut capacity.

In conclusion, raising the  $a/d$  ratio to 1.25 considerably lowered the contribution of the arch action mechanism, as indicated by reduced values for diagonal strain.



**a)** load diagonal concrete strain response for specimen  $a/d=1$



b) load diagonal concrete strain response for specimen  $a/d=1.25$

**Figure 6.** Concrete compression strains

#### 4.4 BFRP Strain

The tensile strain of longitudinal BFRP bars for all tested corbel specimens is presented in **Figure 7**. It is obvious that the reinforcement ratio and shear span-to-depth ratio ( $a/d$ ) significantly influence the strain behavior and failure mode.

In group with an  $a/d$  ratio of 1, specimen C30-R1-pb1-F reached an ultimate strain of  $21,978 \mu\epsilon$ , initially failing by flexural rupture of the BFRP bars, reaching to ultimate tensile strength, followed by concrete crushing. With the increased reinforcement ratio, the strain value decreased, with specimen C30-R1-pb1.57-F reaching  $17,616 \mu\epsilon$ , specimen C30-R1-pb3.15-F strain observed  $10,969 \mu\epsilon$ , and specimens C30-R1-pb5.6-F about  $7,964 \mu\epsilon$ . This reduction in strain corresponded to a transition in failure mode from flexural failure (F) to diagonal compression (DC) failure. The observation aligned with Abu-Obaida et al. 2018, who indicated that the over-reinforced GFRP concrete corbels typically failed by diagonal splitting failure rather than FRP bars rupture.

With an  $a/d$  ratio of 1.25, specimen C30-R1.25-pb1-F recorded an ultimate strain of  $20,752 \mu\epsilon$ . Increasing reinforcement ratio measured the reduction the strain value,

specimen C30-R1.25-pb1.57-F exhibited  $17,181 \mu\epsilon$ , C30-R1.25-pb3.15-F showed  $18,886 \mu\epsilon$ , and C30-R1.25-pb5.6-F reached  $5,353 \mu\epsilon$ . The first specimen in this group exhibited flexure rupture of BFRP bars, subsequently transitioned to DC failure, and splitting failure at a high reinforcement ratio of BFRP. By increasing the  $a/d$ , the stiffness of the concrete corbel decreased, which was reflected in higher strain values observed in the BFRP rebar. The strain response of the BFRP rebars exhibited two distinct stages: initial linear elastic stage, where strain increased proportionally with applied load, indicating inelastic behavior, followed by a non-linear stage characterized by reduced stiffness and significant strain increments for smaller load increases. This observation, integrated with the finding of (Abu-Obaida et al., 2018) showed that high strain values measured by increasing  $a/d$  with different reinforcement ratios resulted in the splitting tensile failure.

Comparing between groups, it was also observed that for the same reinforcement ratio, the specimens with the larger  $a/d$  with slightly larger strain values in the BFRP bars. For instance, both C30-R1-pb3.15-F and C30-R1.25-pb3.15-F shared the same reinforcement but different strain values:

10,969  $\mu\epsilon$  and 18,886  $\mu\epsilon$ , respectively. Longer shear span in the  $a/d = 1.25$  specimens reduced the effect of arching action and increased the contribution of the tie mechanism, thereby subjecting more strain to the BFRP bars.

These test results were integrated into (Dang et al., 2024) It was observed that in GFRP-reinforced corbels. And in deep beams had the same load transfer mechanisms as corbels, increasing  $a/d$  results in increased tie forces and greater FRP strains, as reported by

(Farghaly and Benmokrane, 2013).

(Andermatt and Lubell, 2013) Indicated that due to the linear-elastic behavior and high tensile strength of FRP bars, failure typically occurs either due to abrupt bar rupture or by DC failure, depending on strut and tie interaction. (Trandafir et al., 2023) also confirmed that increasing the FRP ratio reduces strain in every bar but may result in greater crack width.

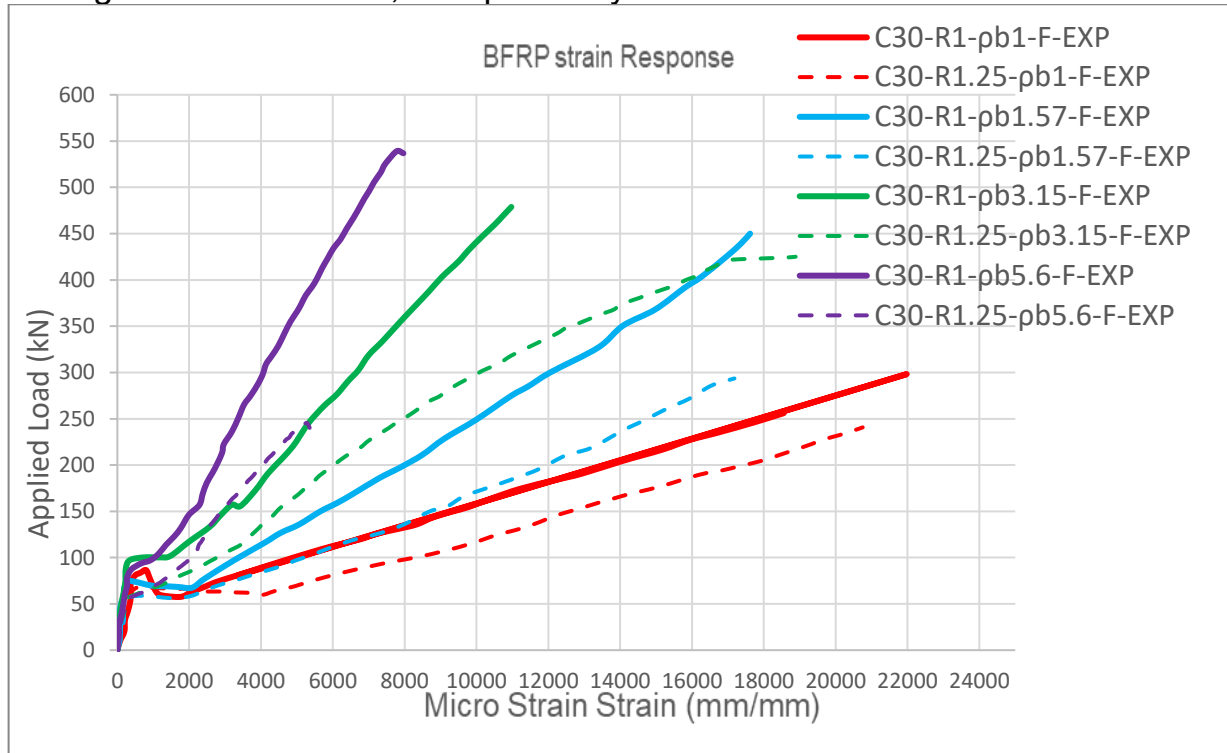


Figure 7. Tensile strain in main BFRP rebars

**5 Analytical Approach**

In order to predict the nominal shear strength of FRP-strengthened concrete corbels, this study used previous analytical equations.

An analytical model presented by (Kim and Jang, 2014) used. The empirical model was initially established through 60 concrete beam tests and is based upon the elastic modulus ratio of FRP bars to steel, shear span-to-depth ratio, and FRP longitudinal reinforcement ratio.

Nominal shear strength equation (1):

$$V_n = \beta_1 \frac{1}{6} \sqrt{f'_c} b d \quad \dots \dots \dots (1)$$

Equation (2) is a correction factor for equation

(1). For  $a/d \leq 2.5$

$$\beta_1 = 3.944 + 0.256 \left( \frac{E_f}{E_s} \right) - 1.472 \left( \frac{a}{d} \right) + 73.886 \rho_f \dots \dots \dots (2)$$

Equation (3) is a correction factor for equation (1). For  $a/d > 2.5$  :

$$\beta_1 = 0.716 + 0.466 \left( \frac{E_f}{E_s} \right) - 0.095 \left( \frac{a}{d} \right) + 32.101 \rho_f \dots \dots \dots (3)$$

$\beta_1$ = Shear strength correction factor

$b$ = width of the section

$d$ = Effective depth of the section

$\frac{a}{d}$  = shear span-to-depth ratio

$\frac{E_f}{E_s}$  = elastic modulus ratio of FRP to steel

$\rho_f$  = longitudinal reinforcement ratio

(Kim and Jang, 2014) introduced a modified regression equation to predict the shear strength of concrete elements by incorporating a shear strength correction factor  $\beta_1$ , as presented in equation (3) and (4). In this study, this equation was further modified to accommodate reinforced concrete corbels reinforced with BFRP bars. The revised formulation, referred to as equation (4) was employed evaluate the proposed shear strength ( $V_{proposed}$ ), the results presented in

**Table 5.**

$$V_n = \beta_1 \frac{1}{6} \sqrt{f'_c} b d \quad \dots\dots\dots (1)$$

$$\beta_f = 124.041 - 194.189 \cdot \left(\frac{E_f}{E_s}\right) - 7.733 \cdot \left(\frac{a}{d}\right) - 1295.750 \cdot \rho_f - 74.488 \cdot \rho_f^2 + 10.943 \cdot \ln(\rho_f) \dots\dots\dots (4)$$

The proposed model demonstrated strong coefficient of determination of  $R^2 = 0.986$ . The results for ( $V_{prop} / V_{exp}$ ) exhibited a strong correlation, with values ranging from 0.87 to 1.27. This indicates a significant relationship in predicting shear strength, particularly with an increase in the reinforcement ratio for both groups with shear span-to-depth ratio a/d of 1 and 1.25. The strong linear correlation between the experimental and predicted shear strength is clearly illustrated in **Figure 8**.

**Table 5.** shear strength of concrete corbel experimental, analytical approach and design proposal

Group	(a/d)	Reinforcement bars	Name	P exp (kN)	( $V_{exp}$ ) (kN)	( $V_{prop}$ ) (kN)	( $V_{prop} / V_{exp}$ )
C30	1	2 No10	C30-R1-pb1-F	400	200	212.71	1.06
		2 No12	C30-R1-pb1.57-F	450.5	225	217.00	0.96
		4 No12	C30-R1-pb3.15-F	478.9	239	266.93	1.12
		4 No16	C30-R1-pb5.6-F	537.0	269	236.03	0.88
	1.25	2 No10	C30-R1.25-pb1-F	290.4	145	131.71	0.91
		2 No12	C30-R1.25-pb1.57-F	255.1	128	136.00	1.06
		4 No12	C30-R1.25-pb3.15-F	427.5	214	185.93	0.87
		4 No16	C30-R1.25-pb5.6-F	244.9	122	155.03	1.27

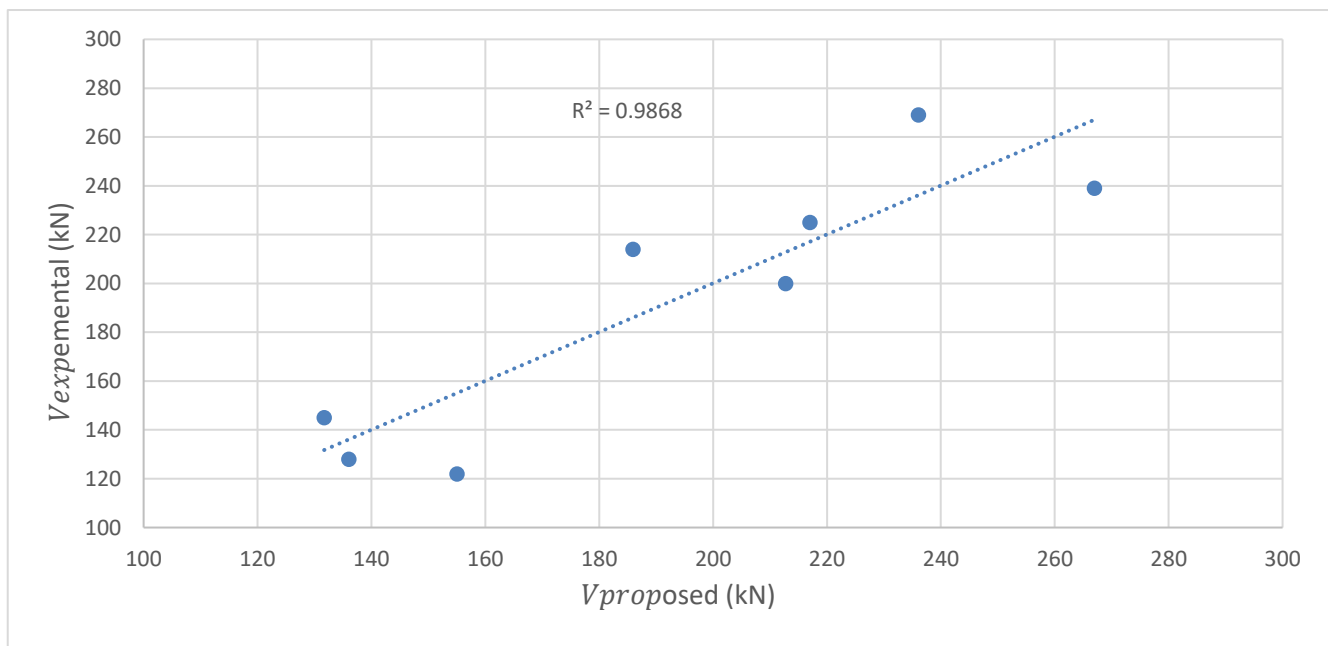


**Figure 8.** Relationship between experimental and proposed shear strength

## 6. Conclusions

The experimental behavior on shear strength of concrete corbels reinforced with BFRP rebar, the study demonstrates the following outcome:

### 1. Load Capacity and Deflection

Increasing the BFRP reinforcement ratio markedly increased shear strength (34.25% higher) and lowered deflection (62% lower) in corbels with an (a/d) ratio of 1.0.

### 2. Failure Mode Transition

Increased reinforcement ratios shifted failure modes from flexural (F) at low reinforcement ratios to diagonal compression (DC) failure. But for high reinforcement ratio change to diagonal splitting (SP) failure at higher ratios.

### 3. Effect of shear span to depth ratio

An increase in shear span-to-depth ratio from a/d = 1.0 to a/d = 1.25 lowered load capacities substantially by about 35–36%, indicative of reduced efficacy in direct arch action under larger shear spans. For increased reinforcement levels at a/d = 1.25, rising reinforcement from 3.15pb to 5.6pb significantly reduced load capacity by approximately 42.7% (from 427.5 kN to 244.9 kN), as brittle splitting failure took over.

### 4. Strain Behavior in BFRP Bars

Increasing the reinforcement ratio led to a reduction in the FRP strain, indicating a shift from reinforcement-controlled failure to concrete-controlled failure. Lower values reached rupture in the BFRP bar with strain  $21,978 \mu\epsilon$  at 1pb, by increasing the reinforcement, lower strains were observed,  $5,353 \mu\epsilon$  at 5.6pb, which reflects a transition from bar rupture-controlled failure to concrete-controlled failure.

### 5. Analytical Approach

The proposed equation ( $V_{\text{proposed}}$ ) provided a modified regression formulation to accurately predict the shear strength of reinforced concrete corbels reinforced with BFRP bars without stirrups. The model demonstrated a high coefficient of determination  $R^2=0.986$ , indicating strong agreement between experimental and predicted results.

6. The results demonstrate that the optimal BFRP reinforcement ratio in a group of a/d of 1 specimen with ratios at 3.15pb and 5.6pb, in the group of a/d of 1.25, at 3.15 ultimate shear strength observed with a change mode of failure in the concrete corbel. That significantly contributed to practical design guidance for engineers, especially in applications requiring corrosion-resistant reinforcement.

7. Furthermore, future research has been suggested, including the long-term durability and performance of BFRP reinforced corbels under environmental stresses and varying loading conditions.

## Reference

- ACI Committee 440 2015. Guide for the design and construction of structural concrete reinforced with fiber-reinforced polymer FRP bars. *ACI Committee 440*. American Concrete Institute.
- Abbood, I. S., Aldeen Odaa, S., Hasan, K. F. & Jasim, M. A. 2021. Properties evaluation of fiber reinforced polymers and their constituent materials used in structures—A review. *Materials Today: Proceedings*, 43, 1003-1008.
- Abu-Obaida, A., El-Ariss, B. & El-Maaddawy, T. 2018. Behavior of short-span concrete members internally reinforced with glass fiber-reinforced polymer bars. *Journal of composites for construction*, 22, 04018038.
- Al-Kamaki, Y. S. S., Hassan, G. B. & Alsofi, G. 2018. Experimental study of the behaviour of RC corbels strengthened with CFRP sheets. *Case Studies in Construction Materials*, 9, e00181.
- Ali, A. Y. & Mahdi, A. M. 2015. ANALYSIS FOR BEHAVIOR AND ULTIMATE STRENGTH OF CONCRETE CORBELS WITH HYBRID REINFORCEMENT. *International Journal of Civil Engineering and Technology (IJCIET)*, Volume 6, Issue 10, Oct 2015, pp. 25-35
- Andermatt, M. F. & Lubell, A. S. 2013. Strength modeling of concrete deep beams reinforced with internal fiber-reinforced polymer. *ACI Structural Journal*, 595.
- Canha, R. M. F., Kuchma, D. A., El Debs, M. K. & De Souza, R. A. 2014. Numerical analysis of reinforced high strength concrete corbels. *Engineering Structures*, 74, 130-144.
- Dang, H. V., Nguyen, S. D., Le, A. V. & Nguyen, D. P. 2024. Experimental Study of the Behavior of GFRP Reinforced Concrete Corbels. *Journal of Materials and Engineering Structures «JMES»*, 11, 361-368.
- Dawood, A. & Abdul-Razzaq, K. S. 2018. Strength of reinforced concrete corbels—a parametric study. *International Journal of Civil Engineering and Technology (IJCIET)*, 9(11), 2018, pp. 2274–2288.
- Farghaly, A. S. & Benmokrane, B. 2013. Shear behavior of FRP-reinforced concrete deep beams without web reinforcement. *Journal of Composites for Construction*, 17, 04013015.

- Kheyroddin, A., Raygan, S. & Kioumars, M. 2024. Strut and tie model for CFRP strengthened reinforced concrete corbels. *Engineering Structures*, 304, 117609.
- Kim, C. H. & Jang, H. S. 2014. Concrete shear strength of normal and lightweight concrete beams reinforced with FRP bars. *Journal of Composites for Construction*, 18, 04013038.
- Lu, W.-Y., Lin, I.-J. & Hwang, S.-J. 2009. Shear strength of reinforced concrete corbels. *Magazine of concrete research*, 61, 807-813.
- Ridha, M. M., Al-Shafi'i, N. T. & Hasan, M. M. 2017. Ultra-high performance steel fibers concrete corbels: Experimental investigation. *Case studies in construction materials*, 7, 180-190.
- Trandafir, A. N., Ernens, G. & Mihaylov, B. I. 2023. Crack-based evaluation of internally FRP-reinforced concrete deep beams without shear reinforcement. *Journal of Composites for Construction*, 27, 04023047.
- Yaseen, S. A. 2020. Flexural Behavior of Self Compacting Concrete T-Beams Reinforced with AFRP. *ZANCO Journal of Pure and Applied Sciences*, 32, 107-114.